



# Insights into the combustion behavior of cork and phloem: effect of chemical components and biomass morphology

Ali Umut Şen<sup>1</sup> · Bruno Esteves<sup>2</sup> · Francisco Lemos<sup>3</sup> · Helena Pereira<sup>1</sup>

Received: 6 August 2022 / Accepted: 6 March 2023

© The Author(s), under exclusive licence to Springer-Verlag GmbH Germany, part of Springer Nature 2023

## Abstract

Thermochemical analysis, wet-chemical analysis, and scanning electron microscopy observations were performed on granulated cork samples of *Quercus cerris* and *Beaucarnea recurvata* and on *Q. cerris* and *Betula pendula* phloems. The results show that the combustion behavior depends both on the chemical composition and the morphology of the bark fractions. The ignition temperature relies on the chemical composition while the combustion rate depends on the morphology and particle size. Ash and suberin contents are positively correlated with ignition and burnout temperatures of cork which vary between 255 and 290 °C, and 500 and 600 °C, respectively. Suberin delays the char oxidation reaction in cork. The average activation energies of cork and phloem are 31.1 and 21.2 kJ mol<sup>-1</sup> in the first and second stages of combustion respectively.

## 1 Introduction

Biomass has been increasingly considered for energy purposes due to environmental and economic reasons, namely for reducing coal-originated greenhouse as well as SO<sub>x</sub> and NO<sub>x</sub> gas emissions, and to valorize underutilized or waste biomass. From a technical point of view, co-combustion of biomass and low-rank coals has shown to be beneficial for improving combustion efficiency (Baxter 2005; Vamvuka and Sfakiotakis 2011; Sahu et al. 2014; Cong et al. 2019), for better control of combustion processes, and for reducing the ash-related problems of biomass combustion (Biagini et al. 2002; Haykiri-Acma and Yaman 2008; Wang et al. 2009; Gil et al. 2010). Co-combustion of biomass with plastics is also considered for a simultaneous reduction of pollution and energy recovery (Colapicchioni et al. 2020).

Bark is among the biomass types that may be used as feedstock in combustion, carbonization, and gasification, although their chemical and fuel-specific properties and

differences in relation to wood advise a detailed characterization and testing (Fengel and Wegener 1984; Sjoström 1993; Rowell 2012). A specific characteristic of bark is the presence of cork and some tree species have cork-rich barks thereby showing different chemical composition and thermal reactivity in relation to the common lignocellulosic materials such as wood, energy crops, and residual bark phloem (Leite and Pereira 2017; Şen and Pereira 2021), given the chemical and structural differences of cork (Fengel and Wegener 1984). With few exceptions, namely the cork from *Quercus suber* which is a valued and widely known industrial raw material (Pereira 2007), most cork-rich bark species are currently underutilized and new valorization routes are investigated to produce sustainable materials including adsorbents, composites, and bio-active extracts, etc. from a circular economy perspective (Şen et al. 2010a, 2012b, 2015, 2016; Lakreb et al. 2018; Şen et al. 2020). The fractionation of cork-rich barks is usually targeted to obtain cork fractions but creates a significant amount of lignocellulosic phloem residues which need to be valorized in view of an overall positive economic balance of their utilization in biorefineries namely by producing value-added products such as biochars (Şen et al. 2016, 2022b). Therefore, thermochemical conversion seems to be a favorable valorization route for such alternative cork species because it allows obtaining a number of high-value-added functional materials, as for example biochar, bio-oil, chemicals, and fuels (Bridgwater 2003, 2010; Brown 2019; Huang et al. 2019). These products have distinctive technical properties and find applications in various

✉ Ali Umut Şen  
umutsen@isa.ulisboa.pt

<sup>1</sup> Forest Research Centre, School of Agriculture, University of Lisbon, Tapada da Ajuda, 1349-017 Lisbon, Portugal

<sup>2</sup> CERNAS Research Centre, Polytechnic Institute of Viseu, 3504-510 Viseu, Portugal

<sup>3</sup> CERENA/Chemical Engineering Department, Instituto Superior Técnico, University of Lisbon, 1049-001 Lisbon, Portugal

industrial fields including as adsorbents, soil amendment materials, solid fuels, electrode materials, and syngas precursors, among others (Şen et al. 2022a, b).

The aim of this work is to investigate the combustion properties of the cork and phloem fractions of cork-rich barks in relation to their differences in chemical composition and morphology by using waste corks obtained from the fractionation of the cork-rich barks of *Quercus cerris* and *Beaucarnea recurvata* and of the residual phloems obtained from the fractionation of *Q. cerris* and *Betula pendula* barks. The current study lays the groundwork for the co-combustion applications of waste cork blends with low-rank coals and waste plastics.

## 2 Materials and methods

### 2.1 Materials

The following waste bark fractions were used in this study, coded as samples A (A1, A2, A3, A3-DS), B, C, and D:

- A. Cork mechanically fractionated from *Q. cerris* bark, as described (Şen et al. 2010a) with three different particle dimensions (A1, A2, and A3 for 420–841  $\mu\text{m}$ , 250–420  $\mu\text{m}$ , and 177–250  $\mu\text{m}$ , respectively) as well as desuberinised *Q. cerris* cork (A3-DS).
- B. Cork (250–420  $\mu\text{m}$ ) separated from the stem of *Beaucarnea recurvata*, as described (Şen et al. 2018).
- C. Phloem (250–420  $\mu\text{m}$ ) separated from the stem of *Q. cerris* bark, as described (Miranda et al. 2013).
- D. Phloem (250–420  $\mu\text{m}$ ) fractionated from *Betula pendula* bark as described (Şen et al. 2010a).

The bark samples were ground with a Retsch 2000 SK Hammer Mill and sieved into different particle fractions of 20–40 mesh (420–841  $\mu\text{m}$ ), 40–60 mesh (250–420  $\mu\text{m}$ ) and 60–80 mesh (177–250  $\mu\text{m}$ ). The detailed chemical characterization of the pure cork samples of the three species can be found elsewhere (Şen et al. 2010a, 2018; Miranda et al. 2013). The chemical composition of *Q. cerris* phloem was previously reported (Şen et al. 2010a).

### 2.2 Chemical analysis

The extractives, suberin, and lignin contents of corks were determined using previously dried samples. Total extractive content was determined by successive Soxhlet extractions according to TAPPI Standards (T204 om-88 and T207 om-93) with dichloromethane, ethanol, and water during 6 h, 18 h, and 18 h extractions for each solvent, respectively. The suberin content was obtained using methanolysis on the extractive-free material (Graça and Pereira 2000). A 1.5 g

extractive-free sample was refluxed with 100 mL of a 3% methanolic solution of  $\text{NaOCH}_3$  for 3 h, filtrated, washed with methanol, refluxed again with 100 mL methanol for 15 min, and filtrated once more. The combined filtrates were acidified to pH 6 with 2 M  $\text{H}_2\text{SO}_4$  and evaporated to dryness. The residues were suspended in 50 mL water and the alcoholysis products recovered with  $\text{CH}_2\text{Cl}_2$  in three subsequent liquid–liquid extractions, with 50 mL  $\text{CH}_2\text{Cl}_2$ . The extracts were dried over anhydrous  $\text{Na}_2\text{SO}_4$ , and the solvent was evaporated. Klason and acid-soluble lignin contents were determined according to TAPPI T 222 om-88 and TAPPI UM 250 Standards on the previously extracted and desuberinised materials.  $\text{H}_2\text{SO}_4$  (72%, 3.0 mL) was added to 0.35 g of the material, placed in a water bath at 30 °C for 1 h and diluted to 4%  $\text{H}_2\text{SO}_4$  and hydrolyzed for 1 h at 120 °C (Sluiter et al. 2008). The detailed procedures for wet chemical analysis can be found elsewhere (Şen et al. 2010a).

### 2.3 Thermogravimetric analysis

Perkin Elmer STA 6000 and TA Instruments SDT 2960 simultaneous DSC-TGA analyzers were used to conduct the thermogravimetric analysis (TGA) of the biomass samples using alumina pans under air or nitrogen flow rates between 20 and 50  $\text{mL min}^{-1}$ . A linear 4-step heating program was applied to the thermogravimetric analyses: in the first step, approximately 5 mg of the samples were kept isothermally at 30–40 °C for 5–10 min for stabilizing the furnace before the non-isothermal runs; a heating step followed until 800 °C with a heating rate of 20 °C  $\text{min}^{-1}$ ; in the third step, the samples were kept isothermal for 5–10 min. at 800 °C; in the last step, the samples were cooled to room temperature with a cooling rate of 50 °C  $\text{min}^{-1}$  (Şen et al. 2022a).

### 2.4 Morphology

Scanning electron microscopy (SEM) observations were performed on cork and phloem samples using a Hitachi S2400 electron microscope under an accelerating voltage of 20.0 kV.

### 2.5 Deconvolution of mass loss rate and heat evolution

The deconvolution of the mass loss rate and heat flow curves of different cork species during combustion was carried out by application of Gaussian or Lorentzian multi-peak fitting.

### 2.6 Proximate analysis

Thermogravimetric analysis between 30 and 800 °C under air and nitrogen flow rates of 20  $\text{mL min}^{-1}$  was performed to

calculate the moisture content, ash content, volatile content, and fixed carbon content of the cork samples.

## 2.7 Determination of combustion parameters

The industrial co-combustion processes require the calculation of combustion indices for the biomass fuels, i.e., ignition ( $D_i$ ), comprehensive combustion indices ( $S$ ), and flammability ( $FI$ ) indices which need the determination of ignition temperature ( $T_i$ ), burnout temperature ( $T_b$ ), and temperature at maximum degradation rate ( $T_p$ ) (Vamvuka and Sfakiotakis 2011; Lu and Chen 2015; Parascanu et al. 2017; Ro et al. 2018).

The ignition index ( $D_i$ ) was calculated by dividing the maximum degradation rate ( $DTG_{max}$ ) by the product of ignition temperature ( $T_i$ ) and temperature at which maximum degradation occurs ( $T_p$ ) (Eq. 1) (Cong et al. 2019).

$$D_i = \frac{DTG_{max}}{T_i \times T_p} \quad (1)$$

The comprehensive combustion index ( $S$ ) was calculated by using maximum and average combustion rates ( $DTG_{max}$  and  $DTG_{avg}$ , respectively) as well as burnout temperature ( $T_b$ ) and the square of ignition temperature ( $T_i$ ) (Eq. 2). The ignition temperature was calculated using the intersection method and the burnout temperature using the conversion method at 99% conversion (Lu and Chen 2015).

$$S = \frac{DTG_{max} \times DTG_{avg}}{T_i^2 \times T_b} \quad (2)$$

The flammability index ( $FI$ ) (Eq. 3) was determined using the maximum combustion rate and ignition temperatures as follows.

$$FI = \frac{DTG_{max}}{T_i^2} \quad (3)$$

## 2.8 Determination of activation energy of char oxidation

A solid-state reaction is commonly described by the following equation based on the assumption that the reaction is dependent on conversion ( $f(\alpha)$ ) and temperature ( $T$ ):

$$\frac{d\alpha}{dt} = A \times e^{-\frac{E_a}{RT}} \times f(\alpha) \quad (4)$$

Here the temperature dependence of the reaction is explained by the Arrhenius equation where  $A$  ( $s^{-1}$ ) is the pre-exponential factor,  $E_a$  is the activation energy ( $\text{kJ mol}^{-1}$ ), and  $R$  is the universal gas constant ( $8.314462 \text{ J mol}^{-1} \text{ K}^{-1}$ ).

The conversion is defined as:

$$\alpha = \frac{m_i - m_t}{m_i - m_f} \quad (5)$$

where  $m_i$  is the initial weight,  $m_t$  is the weight at time  $t$ , and  $m_f$  is the final weight.

Under linear heating conditions, Eq. 4 can be written as follows by introducing the heating rate ( $\beta = dT/dt$ ).

$$\frac{d\alpha}{dT} = \frac{A}{\beta} \times e^{-\frac{E_a}{RT}} \times f(\alpha) \quad (6)$$

The integral form of this equation (Eq. 6) is written as:

$$g(\alpha) = \int_0^\alpha \frac{d(\alpha)}{f(\alpha)} = \frac{A}{\beta} \int_{T_0}^T e^{-E_a/RT} \times dT \quad (7)$$

Since this integral has no exact solution, a numerical method is required to calculate an approximate solution. Among the numerical methods, the Coats-Redfern method uses a Taylor series expansion and is widely used for solid-state kinetic analysis of different materials (Ding et al. 2022). Reaction order, contracting volume/area, diffusion, and reaction models are commonly used for the solid-state reaction model  $f(\alpha)$ . In the present study, the Coats-Redfern method with the first-order kinetic model is selected after comparing the correlation coefficients of different reaction models (Ding et al. 2022).

## 3 Results and discussion

### 3.1 The effect of particle size and chemical composition on combustion behavior of cork

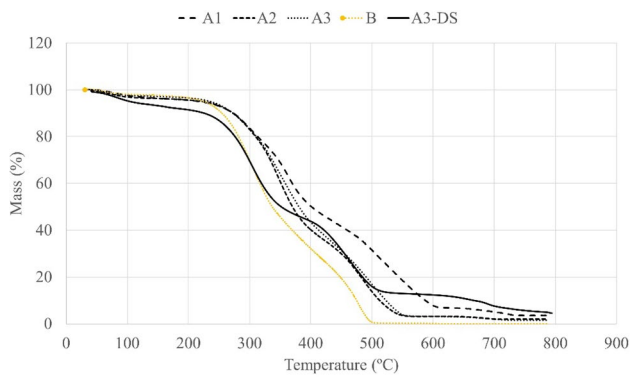
Particle size is an important parameter in combustion as it affects the thermal decomposition rate due to heat transfer limitations within the biomass particles. This effect is clear in cork with different particle sizes (Fig. 1) because mass-loss curves shift to lower temperatures as the particle size decreases from 420  $\mu\text{m}$  (A1–A2), indicating an increased combustion efficiency.

Figure 1 also shows that the combustion behavior of the cork samples differs between species. *Q. cerris* cork (A-samples) degrades at higher temperature than *B. recurvata* cork (B sample).

The different thermal degradation patterns may be linked with differences in the chemical composition and morphology of both cork species (Şen et al. 2016; Leite and Pereira 2017).

Chemical differences include inorganic (ash), extractive, polysaccharide, suberin, and lignin contents (Pereira 1988).

Ash content shows a decreasing pattern with particle size reduction in *Q. cerris* cork (Sen et al. 2020) and the lower



**Fig. 1** Effect of particle size and cork species on mass loss patterns of *Quercus cerris* (A1, A2, A3 and A3-DS) and *Beaucarnea recurvata* (B) corks during combustion. Particle size: A1: 20–40 mesh, A2: 40–60 mesh, A3: 60–80 mesh, B: 40–60 mesh. DS: desuberinized

ash content in the fine fraction of corks is confirmed by the final weight shown in Fig. 1. The particle-size dependence of chemical composition is related to the cellular heterogeneity of bark tissues which have distinct mechanical properties leading to different scission effects during grinding. As a result, certain tissues reduce to fines while others resist leading to different chemical compositions in different fractions. Ash contents linked with these tissues also show variation.

Low molecular-weight extractive compounds possibly contribute to the volatile content and thus to the reactivity of cork. When the volatile content of the solid fuel increases, the fuel reactivity usually increases by decreasing ignition and/or burnout temperatures and increasing combustion rate (Zhang et al. 2006; Chao et al. 2016). *B. recurvata* cork (B) contains higher extractive contents followed by the fine (60–80 mesh) fraction of *Q. cerris* cork (A3) (18% and 14%, respectively) (Fig. 2). Interestingly, these corks are more reactive in combustion as determined by the following combustion parameters analysis.

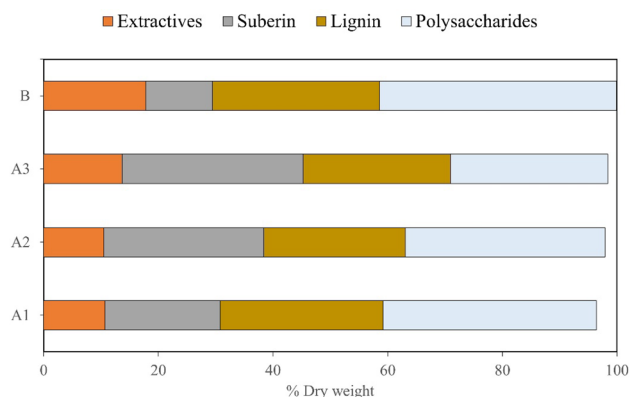


**Fig. 2** Chemical composition of the organic fraction (extractives, polysaccharides, suberin, and lignin) of the corks from *Beaucarnea recurvata* (B) and *Quercus cerris* (A1, A2 and A3)

The proximate analysis demonstrated that the *Q. cerris* and *B. recurvata* corks have quite similar volatile contents (approximately 80–84%) (Fig. 3). This proximate composition is also similar to that of *Q. suber* cork (Atanes et al. 2012). For practical co-combustion applications, one may conclude that since the volatile contents in all the studied corks are higher than 35%, they may be used in the co-combustion of low-rank coals (Biagini et al. 2002). Possibly hemicelluloses and cellulose, as well as a small fraction of lignin which decomposes at lower temperatures, contribute to the volatile content of cork (Şen et al. 2012a, 2014).

Suberin and lignin are considered heat-resistant components of cork contrary to thermally favorable polysaccharides (Şen et al. 2014). Lignin has previously been shown to undergo complete combustion at higher temperatures than xylan and cellulose (Dorez et al. 2014). Lignin content is higher in *B. recurvata* cork (29.2%) while suberin content is higher in the fine *Q. cerris* cork (31.5%), decreasing for bigger particle sizes (Fig. 2). This result suggests that differences in chemical composition between the corks are not sufficient to explain the different combustion behaviors of the corks.

The cork samples undergo combustion reactions in two stages (devolatilization and char oxidation stages, respectively) at lower and higher temperatures between 200–350 and 350–750 °C, respectively, independent of particle size differences (Fig. 4). This behavior is common for different lignocellulosic biomass, although, for forest residues, the second stage usually ends at lower temperatures, for example 600 °C (Vamvuka and Sfakiotakis 2011).

The trimodal degradation pattern of *Q. cerris* cork at the higher temperature stage was also interesting. *Q. cerris* cork shows three major combustion peaks (excluding the water evaporation peak) at temperatures of 350–375 °C, 490–530 °C, and 700–720 °C. The additional third peak at

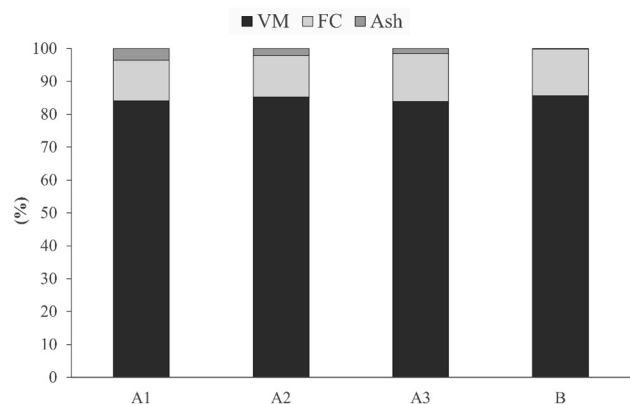


**Fig. 3** Proximate analysis of *Quercus cerris* (A1, A2, A3) and *Beaucarnea recurvata* (B) corks. VM volatile matter, FC fixed carbon, Ash inorganic matter

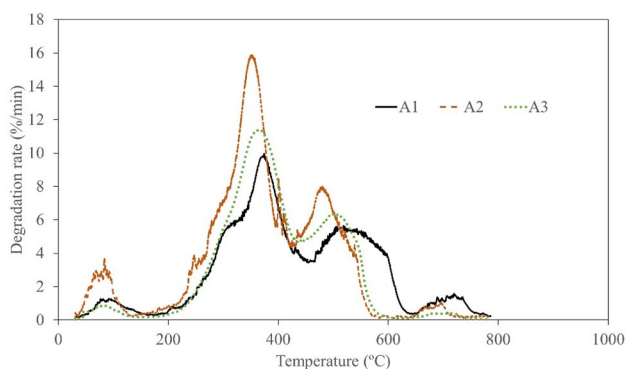


**Fig. 4** Effect of particle size on the combustion rate of *Quercus cerris* cork. Particle size: A1: 20–40 mesh, A2: 40–60 mesh, A3: 60–80 mesh

a high temperature implies that the char of *Q. cerris* cork has a heterogeneous structure with a different reactivity at moderate and high temperatures.

The combustion patterns may also be evaluated by the combustion reactions of polysaccharides and lignin, and of the remaining lignin and char, respectively (Vamvuka and Sfakiotakis 2011). According to a previous study (Wang et al. 2020), lignin content plays a role in the ignition mechanism, while cellulose content is likely to determine the ignition temperature of biomass. In agreement with Wang et al. (2020), the cellulose content was shown to favor the pyrolysis rate (Gani and Naruse 2007).

Interestingly, the ignition of hemicelluloses was found to be similar to that of cellulose (Wang et al. 2020).

The shapes of DTG curves (Fig. 4) allow important insights into the chemical composition of the different granulometric fractions i.e., the presence or absence of a particular peak may be linked with a chemical component, which is in agreement with our previous results (Şen et al. 2020). In order to better analyze the DTG curves, peak deconvolutions were performed considering pseudocomponent (PS) peak distributions (Fig. 5). The presence of a shoulder approximately at 300 °C and the irregular shape of the second stage peak at 580 °C in bigger cork particles (A1-Peak2 and Peak5) are assigned to hemicelluloses which possibly have a lower content in the smaller fraction (A3-no distinct peak).

The devolatilization starts at 150 °C and reaches its maximum value around 380 °C while char oxidation starts at approximately 380 °C. The overall thermal degradation of cork can be modeled as multiple parallel reactions. These reactions possibly correspond to the elimination of moisture, degradation of hemicelluloses, degradation of cellulose, and char oxidation reactions in three stages. A significant part of the suberin and a small fraction of lignin possibly degrade during devolatilization. Interestingly, when the cork is desuberinised, char oxidation starts at lower temperatures (380 °C vs 340 °C) showing the heat-protective properties of suberin (Fig. 5) (Şen et al. 2014).

An interesting result is the second reaction rate at approximately 710 °C (Fig. 5). It is higher in cork with less suberin

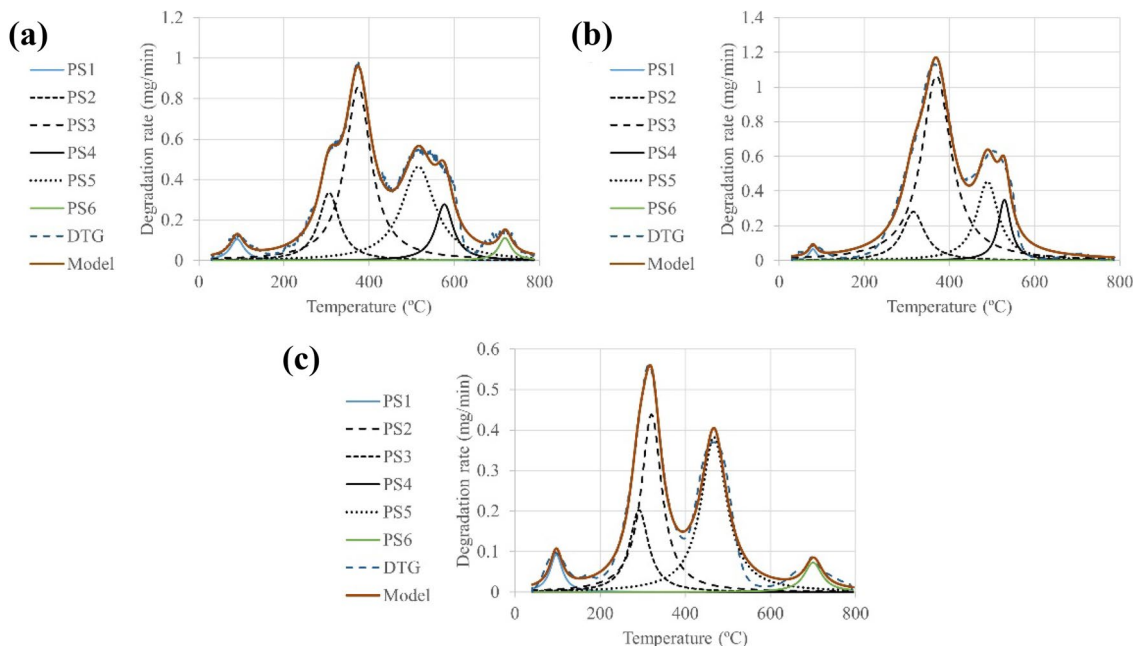


**Fig. 5** Deconvolution of the combustion rate peak for *Quercus cerris* cork: **a** A1: 20–40 mesh, **b** A3: 60–80 mesh; **c** A3-DS: 60–80 mesh and desuberinised). PS pseudocomponents

content (A1) and desuberinised cork (A3-DS) compared with high suberin-containing cork (A3). This result suggests that the second reaction is possibly lignin-related with lignin being the main component responsible for heat resistance at higher temperatures while suberin provides heat resistance at lower temperatures.

The analyzed corks were obtained from cork-rich barks by grinding them followed by the size and density separation of the cork and phloem fractions (Şen et al. 2016). Therefore, the cork fractions still contain phloem impurities that will impact their thermal behavior, given the chemical differences between cork and phloem (Şen et al. 2010a). Consequently, the characterization of the combustion behavior of phloem helps in understanding the combustion characteristics of corks as shown in the following section along with the results of cork.

### 3.2 Combustion characteristics of cork and phloem

The combustion characteristics of cork and phloem samples were compared by determination of specific combustion temperatures and calculation of combustion indices and activation energy in char oxidation. The specific combustion temperatures of the different cork and phloem samples are shown in Table 1. The ignition temperatures vary between 255 and 290 °C for cork samples. These temperatures are similar to the values reported for cork (Blázquez et al. 2019) but higher than those obtained for agricultural and forestry wastes, although a note of caution is due here because particle size affects the ignition temperature (Vamvuka and Sfakiotakis 2011). On the other hand, the ignition temperatures of low-rank coals are reported to vary between 273 and 412 °C (Vamvuka and Sfakiotakis 2011; Cong et al. 2019). These results indicate that corks have ignition temperatures in the lower range of low-rank coals. *Q. cerris* corks show the highest

ignition temperatures which did not significantly change between different particle sizes while *B. recurvata* cork has the lowest ignition temperature. On the other hand, phloem samples of *Betula pendula* and *Q. cerris* showed slightly lower ignition temperatures than cork (Table 1). These differences in ignition temperature possibly arise from their difference in chemical composition, particularly due to their polysaccharide contents (Şen and Pereira 2021) which is in agreement with Wang et al. (2020). A peculiar result was the reduction of the ignition temperature in desuberinised cork (290 °C vs 260 °C) which further shows the role of suberin in combustion. The overall results suggest that the ignition temperature of cork possibly depends on the competing favorable and unfavorable effects of polysaccharides and suberin.

The burnout temperatures of the different corks vary between 500 and 600 °C, which is in agreement with values obtained for cork and other biomass types (Vamvuka and Sfakiotakis 2011; Blázquez et al. 2019). Interestingly desuberinisation increased the burnout temperature to a considerable extent (approximately 200 °C). The char oxidation reaction (Fig. 5) and the possible involvement of lignin in desuberinised cork are likely to promote a slowing of the char oxidation at lower temperatures. This result has a particular significance for the usage of this material for high-temperature insulation.

The burnout temperatures of cork samples are lower than low-rank coal except for desuberinised cork (Vamvuka and Sfakiotakis 2011), and among the cork species *B. recurvata* cork has the lowest burnout temperature. The burnout temperature of *Q. cerris* cork decreases at particles smaller than 420 µm particle size.

Another interesting result was the higher thermal resistance of phloem than cork at higher temperatures as may be verified by the highest burnout temperatures of *B. pendula* and *Q. cerris* phloems (Table 1). This result suggests

**Table 1** Combustion properties of cork and phloem

Biomass	$T_i$ (°C)	$T_b$ (°C)	$T_m$ (°C)	$DTG_{max}$ (% min <sup>-1</sup> )	$D_i$ ( $\times 10^{-5}$ )	$S$ ( $\times 10^{-7}$ )	$FI$ ( $\times 10^{-5}$ )	$E_a$ -first stage (kJ mol <sup>-1</sup> )
A1	285	600	374	9.95	9.33	5.48	12.26	26.01
A2	290	550	350	15.86	15.63	10.60	18.86	27.83
A3	290	550	364	11.39	10.77	6.33	13.54	32.71
A3-DS	260	756	305	11.14	14.10	4.36	16.6	27.48
B	255	500	424	26.30	24.30	39.51	40.50	48.51
C	260	743	700	3.42	1.84	0.28	4.87	24.46
D	265	585	368	11.46	11.80	9.53	16.30	27.36
Low-rank coals [1, 2, 49, 50]	273–412	739	–	–	–	–	–	88–90

$T_i$  ignition temperature,  $T_b$  burnout temperature,  $T_m$  maximum degradation temperature,  $DTG_{max}$  maximum combustion rate,  $D_i$  ignition index,  $S$  comprehensive combustion index,  $FI$  flammability index,  $E_a$  activation energy

that phloem residues obtained from cork processing are not likely to improve the co-combustion performance of low-rank coals but they could be used as low-temperature thermal insulation coatings in construction, a similar use to that was proposed for high-ash containing rice husks (Gonçalves and Bergmann 2007; Muthuraj et al. 2019).

The combustion indices show that *B. recurvata* cork is more reactive than *Q. cerris* cork with its significantly higher ignition, comprehensive combustion, and flammability indices. This result suggests that *B. recurvata* cork has a higher potential for co-combustion applications than *Q. cerris* cork. Although a possible interference of noise in the DTG signal cannot be ruled out in these calculations which may affect the results of combustion indices, these results allow a comparison of the combustion behavior of different corks.

Another interesting parameter in combustion is time analysis, i.e., analysis of ignition ( $t_i$ ) and maximum degradation ( $t_m$ ) times. Interestingly corks attain ignition and maximum degradation times between 13 and 20 min, while *Q. cerris* phloem ignites earlier than cork but its maximum degradation occurs belatedly (Fig. 6) possibly because of the effect of chemical composition, i.e., its higher lignin and ash contents (Şen et al. 2010b). This result has practical implications in the preparation of coating materials for thermal insulation.

The variation of combustion indices between the different corks and particle sizes suggests that the anatomical structure of the cork is likely to play an important role in oxygen transport and therefore in the combustion properties of corks.

For the comparison of the differences in the anatomical structure of cork and phloem, the extensive work made on the structural aspects of cork from *Q. suber* (Pereira 2007) may be taken as a reference where cork cells are modeled as regular hexagonal prisms and the volume of cork cells is

approximated by a simple formula based on cell biometric measurements in the following equation (Eq. 8):

$$V_p = \frac{3\sqrt{3}}{2} \times a^2 \times h \quad (8)$$

where  $a$  is the base edge and  $h$  is prism height (Pereira 2007).

The volumes of cork cells calculated by this method show that *B. recurvata* cork cells are 35 times greater than those of *Q. suber* cork cells and 48 times greater than those of *Q. cerris* cork cells (Şen et al. 2011, 2018). Thus, *B. recurvata* cork being composed of larger cells (Şen et al. 2018) possibly favor oxygen transport and facilitate combustion. This result is in accordance with a previous study (Gani and Naruse 2007) suggesting that the morphology of biomass, in particular, of the char, is closely related to the combustion reactivity of the biomass. The surface morphology of the cork and phloem samples is shown in Fig. 7. The clear difference between the cork and phloem is apparent with cork samples (A2 and B) shown as cellular prisms while phloem (C and D) samples are shown as more compact materials. The structure of the phloem is likely to delay the gas transport during the devolatilization and char oxidation stages and thus decreases the combustion rate.

The activation energy of cork and phloem in combustion ranged between 24.5 and 48.5 kJ mol<sup>-1</sup> (Table 1). The average activation energies in the two combustion stages were 31.1 and 21.2 kJ mol<sup>-1</sup> (Table 2) which were approximately one-third of the low-rank coals (Taş and Yürüm 2012; Engin and Atakül 2018). The desuberinisation decreased the activation energy in the first stage. Phloem samples showed in general lower activation energies than cork samples (Tables 1, 2). The low activation energies of cork and phloem samples are different than wood activation energy values which have shown to be higher than that of coals (Taş and Yürüm 2012). This result has an important implication in co-combustion that blending of cork or phloem with low-rank coals is likely to decrease the overall activation energy favoring the co-combustion (Guo and Zhong 2018). Different cork/phloem and low-rank coal blending ratios should be tested for this task, which is beyond the scope of this study.

The heat release profiles also provide important insights into the combustion of cork and phloem (Fig. 8). The DSC peaks almost overlapped the DTG peaks confirming the two-stage (devolatilization and char oxidation) reactions in cork. Interestingly, *Q. cerris* and *B. recurvata* corks had similar exothermic heat release patterns with two exothermic peaks at temperatures of approximately 370 °C and 470 °C, although they have different chemical compositions which further suggests the dependence of combustion behavior of cork both on chemical composition and biomass morphology.

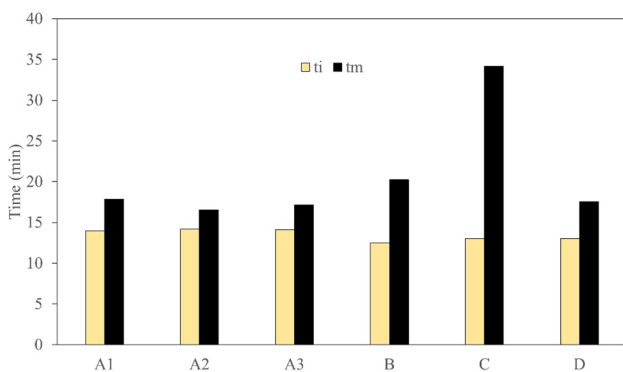


**Fig. 6** Comparison of ignition ( $t_i$ ) and maximum degradation ( $t_m$ ) times of different species. A1–A3: *Quercus cerris* cork, B: *Beaucarnea recurvata* cork, C: *Quercus cerris* phloem, D: *Betula pendula* phloem

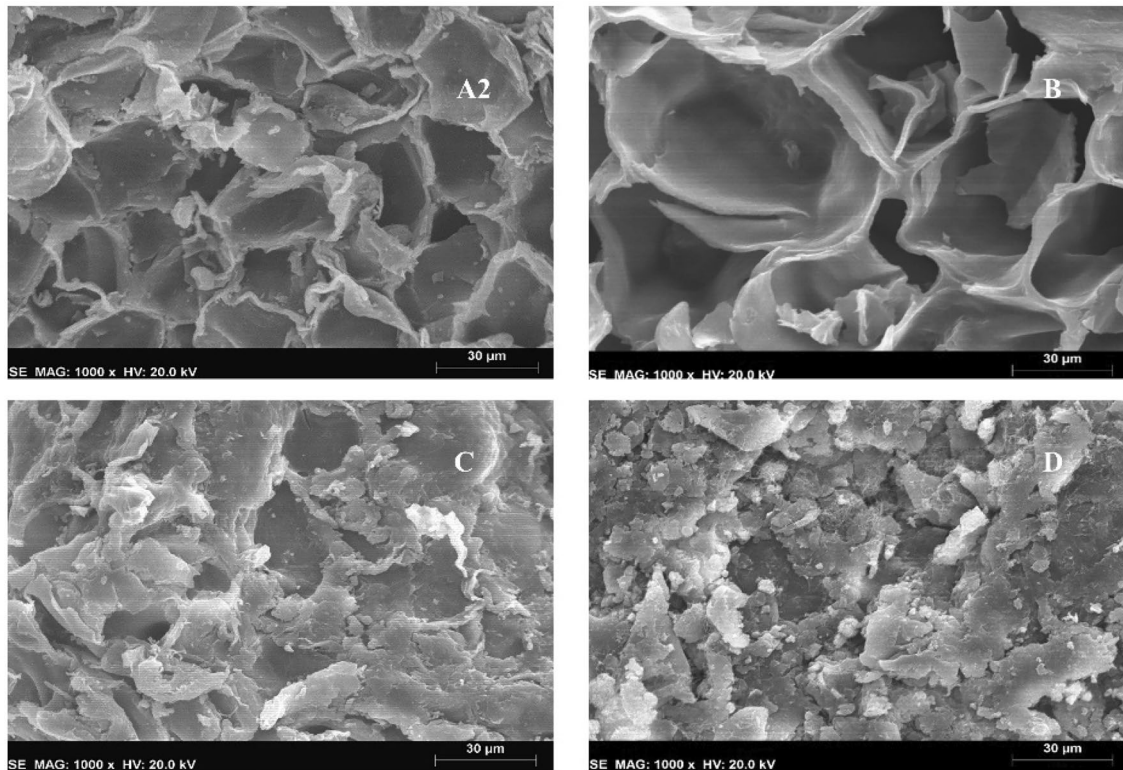


**Fig. 7** Morphological differences between *Quercus cerris* and *Beaucarnea recurvata* corks (A2, B) and *Quercus cerris* and *Betula pendula* phloems (C, D)

**Table 2** Variation of activation energy  $E_a$  during combustion stages in different cork and phloem fractions

Biomass	Temperature range (°C)	$E_a$ (kJ mol <sup>-1</sup> )	R <sup>2</sup>
A1	200–320	26.01	93.01
	380–520	11.85	95.50
A2	200–320	27.83	92.30
	380–520	23.57	90.62
A3	200–320	32.71	96.31
	380–520	22.28	95.82
A3-DS	200–320	27.48	92.48
	380–520	24.37	93.70
B	200–320	48.51	98.06
	380–520	47.27	85.03
C	200–320	24.46	86.15
	380–520	9.25	83.18
D	200–320	27.36	88.07
	380–520	12.81	95.99
Average	200–320	31.14	–
	380–520	21.17	–

A striking difference in heat release profiles between the *Q. cerris* (A2) and *B. recurvata* (B) corks was the contribution of the exothermic peaks as evaluated by the area ratios of the deconvoluted exothermic peaks (Fig. 9). The first peak contributes approximately 62% of exothermic heat release in *Q. cerris* cork while in *B. recurvata* cork, the first peak contributes approximately 88% of exothermic heat release. This result implies that both the chemical composition and morphology affect the combustion reactions in cork with the chemical composition being particularly significant in the devolatilization process while the morphology or individual cell dimensions play an important role both in devolatilization and in char oxidation.

In addition to biomass morphology, the cork particle size also influences the heat release due to heat transfer. As the particle size decreases, the heat release curves shift to lower temperature, and the amount of heat release increases. In a previous study with *Q. cerris* cork using the heating rate of 5 °C min<sup>-1</sup>, the peak temperatures in the first and second reaction zones were approximately 40 °C lower (Şen et al. 2014). Thus, increasing the heating rate shifts the peak temperatures to higher temperatures.

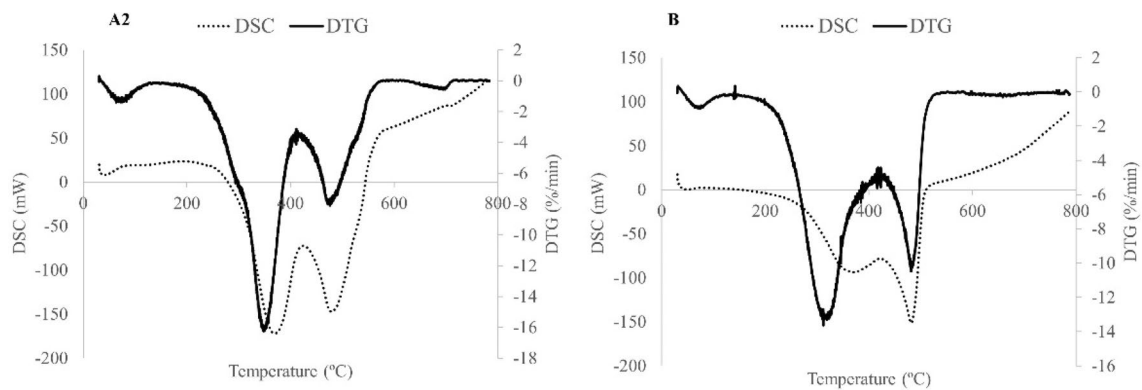


**Fig. 8** Heat flow patterns during combustion of corks of *Quercus cerris* (**A2**, on the left) and *Beaucarnea recurvata* (**B**, on the right)

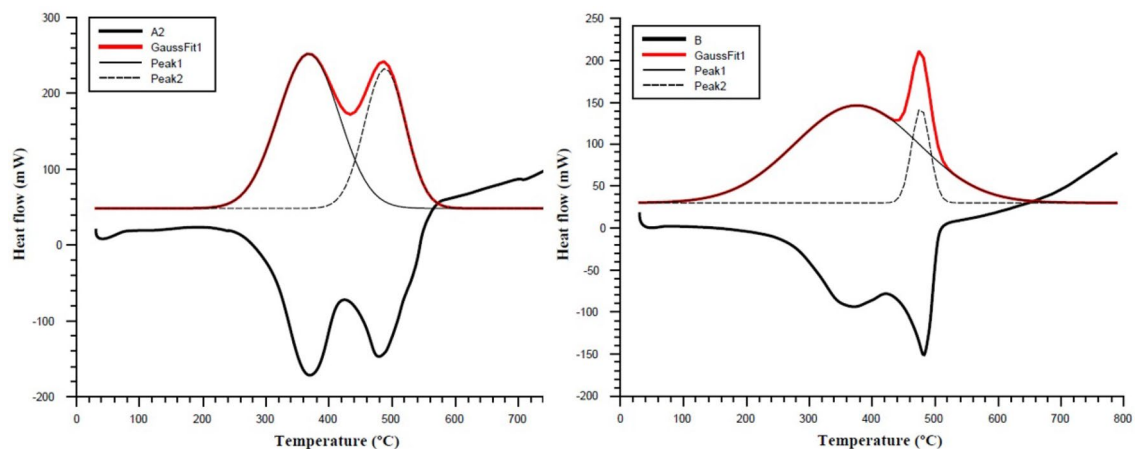


**Fig. 9** Deconvolution of heat release curves of *Quercus cerris* (**A2**, on the left) and *B. recurvata* (**B**, on the right) corks

### 3.3 Correlations between combustion temperatures, activation energy, and biomass composition

The evaluation of the specific combustion temperatures, activation energy, and biomass composition gives insights into how these parameters relate to each other (Fig. 10). The ignition temperature ( $T_i$ ) has a strong correlation with suberin content (Pearson correlation coefficients of 0.90). On the other hand, the ignition temperature has strong negative correlations with extractive content and activation energy in the first stage (Pearson correlation coefficients of  $-0.87$  and  $-0.92$ , respectively) (Fig. 10a). The burnout temperature ( $T_b$ ) has a very high correlation with ash content (Pearson correlation coefficient of 0.99) and strong negative correlations with activation energy and extractive content (Pearson correlation coefficients of  $-0.90$  and  $-0.85$ , respectively) (Fig. 10b). The maximum degradation temperature ( $T_m$ ) has strong correlations with the activation energy, extractive, and lignin contents (Pearson correlation coefficients of 0.90, 0.88, and 0.86,

respectively) (Fig. 10c). The maximum degradation rate ( $DTG_{max}$ ) has strong correlations with the volatile matter, activation energy, and extractive contents (Pearson correlation coefficients of 0.91, 0.90, and 0.80, respectively). The maximum degradation rate has a strong negative correlation with ash content (Pearson correlation coefficient of  $-0.86$ ) (Fig. 10d). These figures suggest that ash and suberin have a negative effect on the combustion properties of cork and the ash and suberin contents may be used to estimate the combustion behavior of different corks.

Another interesting correlation is the relationship between the activation energy and the composition of the corks (Fig. 10e). Surprisingly, the activation energy showed a strong correlation with the extractive content of cork (Pearson correlation coefficient of 0.98) and a strong negative correlation (Pearson correlation coefficient of  $-0.92$ ) with the ash content of cork. This result suggests that different cork species may be screened for extractive and ash contents to estimate the activation energy of cork in combustion.

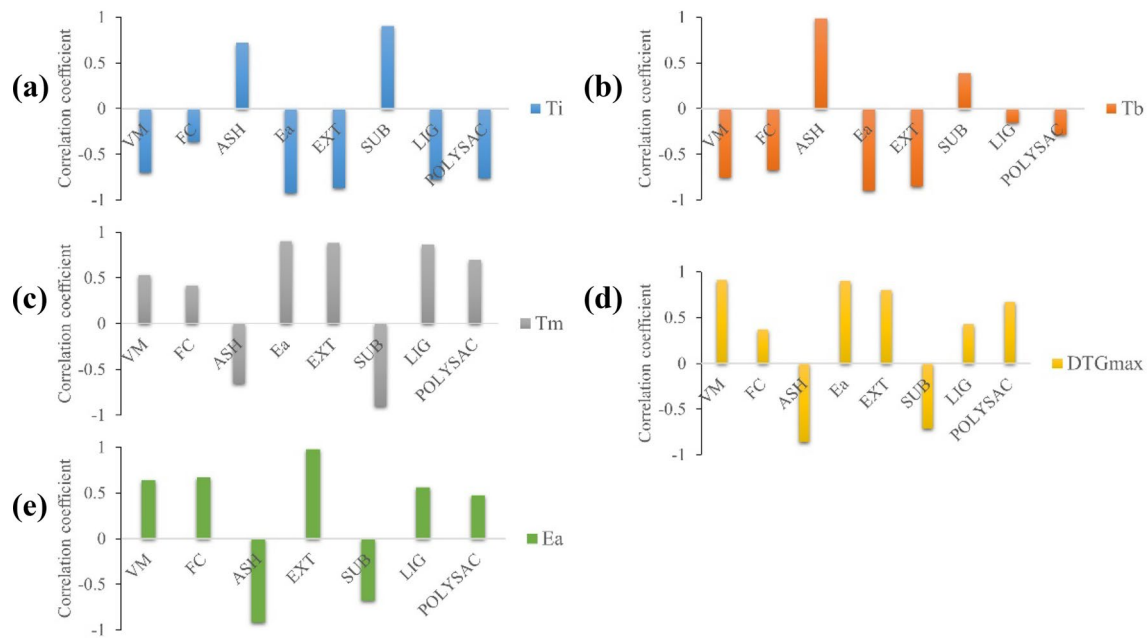


**Fig. 10** Correlation coefficients between specific combustion parameters and composition of cork.  $T_i$  the ignition temperature,  $T_b$  the burn-out temperature,  $T_m$  the maximum degradation temperature,  $DTG_{max}$  the maximum degradation rate,  $VM$  volatile matter,  $FC$  fixed carbon,

$ASH$  inorganic matter,  $Ea$  activation energy,  $Ext$  extractive content,  $Sub$  suberin content,  $Lig$  lignin content,  $Polysac$  polysaccharide content

## 4 Conclusion

Comparative combustion characteristics of *Q. cerris* and *Beaucarnea recurvata* corks and *Q. cerris* and *Betula pendula* phloem were investigated for the first time. The following conclusions can be drawn from the study:

1. Combustion of cork occurs in two main stages: devolatilization and char oxidation. The char oxidation stage occurs in different sub-stages in different corks depending on their chemical composition and morphology.
2. The polysaccharide content is likely to affect the ignition temperature and char oxidation reaction while morphology and particle size affect the combustion rate.
3. Suberin delays the char oxidation reaction in cork.
4. Suberin and ash negatively affect the combustion parameters of cork while volatiles and extractives favor them.

**Acknowledgements** Forest Research Centre (CEF) is a research unit funded by Fundação para a Ciência e a Tecnologia (FCT) (UIDB/00239/2020). The first author acknowledges support from FCT through a research contract (DL 57/2016). A. Umut Şen thanks Isabel Nogueira from Instituto Superior Técnico for her kind help in SEM analysis.

**Author contributions** A.U.S. wrote the main manuscript text and prepared figures and tables. B.E., F.L., and H.P. reviewed and edited the manuscript.

**Data availability** All data generated or analyzed during this study are included in this published article.

## Declarations

**Conflict of interests** The authors declare no competing interests.

## References

- Atanes E, Nieto-Márquez A, Cambra A et al (2012) Adsorption of  $SO_2$  onto waste cork powder-derived activated carbons. *Chem Eng J* 211:60–67
- Baxter L (2005) Biomass-coal co-combustion: opportunity for affordable renewable energy. *Fuel* 84:1295–1302
- Biagini E, Lippi F, Petarca L, Tognotti L (2002) Devolatilization rate of biomasses and coal–biomass blends: an experimental investigation. *Fuel* 81:1041–1050
- Blázquez G, Pérez A, Ianez-Rodríguez I et al (2019) Study of the kinetic parameters of thermal and oxidative degradation of various residual materials. *Biomass Bioenergy* 124:13–24
- Bridgwater AV (2003) Renewable fuels and chemicals by thermal processing of biomass. *Chem Eng J* 91:87–102
- Bridgwater AV (2010) Fast pyrolysis of biomass for energy and fuels. In: Crocker M (ed) *Thermochemical conversion of biomass to liquid fuels and chemicals*. Royal Society of Chemistry, pp 146–191
- Brown RC (2019) *Thermochemical processing of biomass: conversion into fuels, chemicals and power*. Wiley, New York
- Chao J, Yang H, Wu Y et al (2016) The investigation of the coal ignition temperature and ignition characteristics in an oxygen-enriched FBR. *Fuel* 183:351–358

- Colapicchioni V, Mosca S, Guerriero E et al (2020) Environmental impact of co-combustion of polyethylene wastes in a rice husks fueled plant: evaluation of organic micropollutants and PM emissions. *Sci Total Environ* 716:135354
- Cong K, Han F, Zhang Y, Li Q (2019) The investigation of co-combustion characteristics of tobacco stalk and low rank coal using a macro-TGA. *Fuel* 237:126–132
- Ding Y, Zhang W, Zhang X et al (2022) Pyrolysis and combustion behavior study of PMMA waste from micro-scale to bench-scale experiments. *Fuel* 319:123717
- Dorez G, Ferry L, Sonnier R et al (2014) Effect of cellulose, hemicellulose and lignin contents on pyrolysis and combustion of natural fibers. *J Anal Appl Pyrolysis* 107:323–331
- Engin B, Atakül H (2018) Air and oxy-fuel combustion kinetics of low rank lignites. *J Energy Inst* 91:311–322
- Fengel D, Wegener G (1984) Wood: chemistry, ultrastructure. *Reactions* 613:1960–1982
- Gani A, Naruse I (2007) Effect of cellulose and lignin content on pyrolysis and combustion characteristics for several types of biomass. *Renew Energy* 32:649–661
- Gil MV, Casal D, Pevida C et al (2010) Thermal behaviour and kinetics of coal/biomass blends during co-combustion. *Bioresour Technol* 101:5601–5608
- Gonçalves MRF, Bergmann CP (2007) Thermal insulators made with rice husk ashes: Production and correlation between properties and microstructure. *Constr Build Mater* 21:2059–2065
- Graça J, Pereira H (2000) Methanolysis of bark suberins: analysis of glycerol and acid monomers. *Phytochem Anal Int J Plant Chem Biochem Technol* 11:45–51
- Guo F, Zhong Z (2018) Optimization of the co-combustion of coal and composite biomass pellets. *J Clean Prod* 185:399–407
- Haykiri-Acma H, Yaman S (2008) Effect of co-combustion on the burnout of lignite/biomass blends: a Turkish case study. *Waste Manag* 28:2077–2084
- Huang Q, Song S, Chen Z et al (2019) Biochar-based materials and their applications in removal of organic contaminants from wastewater: state-of-the-art review. *Biochar* 1:45–73
- Lakreb N, As N, Gorgun V et al (2018) Production and characterization of particleboards from cork-rich *Quercus cerris* bark. *Eur J Wood Prod* 76:989–997. <https://doi.org/10.1007/s00107-017-1284-6>
- Leite C, Pereira H (2017) Cork-containing barks—a review. *Front Mater* 3:63
- Lu J-J, Chen W-H (2015) Investigation on the ignition and burnout temperatures of bamboo and sugarcane bagasse by thermogravimetric analysis. *Appl Energy* 160:49–57
- Miranda I, Gominho J, Mirra I, Pereira H (2013) Fractioning and chemical characterization of barks of *Betula pendula* and *Eucalyptus globulus*. *Ind Crops Prod* 41:299–305
- Muthuraj R, Lacoste C, Lacroix P, Bergeret A (2019) Sustainable thermal insulation biocomposites from rice husk, wheat husk, wood fibers and textile waste fibers: elaboration and performances evaluation. *Ind Crops Prod* 135:238–245
- Parascanu MM, Sandoval-Salas F, Soreanu G et al (2017) Valorization of Mexican biomasses through pyrolysis, combustion and gasification processes. *Renew Sustain Energy Rev* 71:509–522
- Pereira H (1988) Chemical composition and variability of cork from *Quercus suber* L. *Wood Sci Technol* 22:211–218
- Pereira H (2007) Cork: biology, production and uses. Elsevier, Radarweg 29, PO Box 211. 1000 AE Amsterdam, The Netherlands
- Ro KS, Libra JA, Bae S et al (2018) Combustion behavior of animal-manure-based hydrochar and pyrochar. *ACS Sustain Chem Eng* 7:470–478
- Rowell RM (2012) Handbook of wood chemistry and wood composites. CRC Press, Boca Raton
- Sahu SG, Chakraborty N, Sarkar P (2014) Coal–biomass co-combustion: an overview. *Renew Sustain Energy Rev* 39:575–586
- Şen AU, Pereira H (2021) State-of-the-art char production with a focus on bark feedstocks: processes, design, and applications. *Processes* 9:87
- Şen A, Miranda I, Esteves B, Pereira H (2020) Chemical characterization, bioactive and fuel properties of waste cork and phloem fractions from *Quercus cerris* L. bark. *Ind Crops Prod* 157:112909
- Şen A, Miranda I, Santos S et al (2010a) The chemical composition of cork and phloem in the rhytidome of *Quercus cerris* bark. *Ind Crops Prod* 31:417–422. <https://doi.org/10.1016/j.indcrop.2010.01.002>
- Şen A, Marques AV, Gominho J, Pereira H (2012a) Study of thermochemical treatments of cork in the 150–400 °C range using colour analysis and FTIR spectroscopy. *Ind Crops Prod* 38:132–138. <https://doi.org/10.1016/j.indcrop.2012.01.018>
- Şen A, Olivella MA, Fiol N et al (2012b) Removal of chromium (VI) in aqueous environments using cork and heat-treated cork samples from *Quercus cerris* and *Quercus suber*. *BioResources* 7:4843–4857
- Şen A, De Melo MMR, Silvestre AJD et al (2015) Prospective pathway for a green and enhanced friedelin production through supercritical fluid extraction of *Quercus cerris* cork. *J Supercrit Fluids*. <https://doi.org/10.1016/j.supflu.2014.12.008>
- Şen A, Leite C, Lima L et al (2016) Industrial valorization of *Quercus cerris* bark: pilot scale fractionation. *Ind Crops Prod* 92:42–49. <https://doi.org/10.1016/j.indcrop.2016.07.044>
- Şen A, Miranda I, Ferreira J et al (2018) Chemical composition and cellular structure of ponytail palm (*Beaucarnea recurvata*) cork. *Ind Crops Prod* 124:845–855
- Şen AU, Fonseca FG, Funke A et al (2022a) Pyrolysis kinetics and estimation of chemical composition of *Quercus cerris* cork. *Biomass Convers Biorefin* 12:4835–4845
- Şen AU, Nobre C, Durão L et al (2022b) Low-temperature biochars from cork-rich and phloem-rich wastes: fuel, leaching, and methylene blue adsorption properties. *Biomass Convers Biorefin* 12:3899–3909
- Şen A, Quilhó T, Pereira H (2011) The cellular structure of cork from *Quercus cerris* var. *cerris* bark in a materials' perspective. *Ind Crops Prod* 34:929–936. <https://doi.org/10.1016/j.indcrop.2011.02.015>
- Şen A, Van Den Bulcke J, Defoirdt N et al (2014) Thermal behaviour of cork and cork components. *Thermochim Acta* 582:94–100. <https://doi.org/10.1016/j.tca.2014.03.007>
- Sjostrom E (1993) Wood chemistry: fundamentals and applications. Gulf Professional Publishing, Academic Press
- Sluiter A, Hames B, Ruiz R et al (2008) Determination of structural carbohydrates and lignin in biomass. *Lab Anal Proc* 1617:1–16
- Taş S, Yürüm Y (2012) Co-firing of biomass with coals: Part 2. Thermogravimetric kinetic analysis of co-combustion of fir (*Abies bornmulleriana*) wood with Beypazari lignite. *J Therm Anal Calorim* 107:293–298
- Vamvuka D, Sfakiotakis S (2011) Combustion behaviour of biomass fuels and their blends with lignite. *Thermochim Acta* 526:192–199
- Wang C, Wang F, Yang Q, Liang R (2009) Thermogravimetric studies of the behavior of wheat straw with added coal during combustion. *Biomass Bioenergy* 33:50–56
- Wang S, Zou C, Lou C et al (2020) Effects of hemicellulose, cellulose and lignin on the ignition behaviors of biomass in a drop tube furnace. *Bioresour Technol* 310:123456
- Zhang L, Huang J, Fang Y, Wang Y (2006) Gasification reactivity and kinetics of typical Chinese anthracite chars with steam and CO<sub>2</sub>. *Energy Fuels* 20:1201–1210

**Publisher's Note** Springer Nature remains neutral with regard to jurisdictional claims in published maps and institutional affiliations.

Springer Nature or its licensor (e.g. a society or other partner) holds exclusive rights to this article under a publishing agreement with the

author(s) or other rightsholder(s); author self-archiving of the accepted manuscript version of this article is solely governed by the terms of such publishing agreement and applicable law.